Journal of Hydrology 651 (2025) 132588

Contents lists available at ScienceDirect

Journal of Hydrology

journal homepage: www.elsevier.com/locate/jhydrol

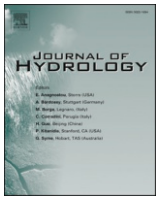

Research papers

Suspended sediment dynamics at the inlets of Venice Lagoon: Unraveling the effects of storm surges and mobile barrier operations

Gian Marco Scarpa [a,*], Silvio Davison [a], Giorgia Manfè [a], Giuliano Lorenzetti [a], Luca Zaggia [b,1], Federica Braga [a,1]

[a] Institute of Marine Sciences - National Research Council (CNR-ISMAR), Castello 2737/F, 30122 Venice, Italy
[b] Institute of Geosciences and Earth Resources - National Research Council (CNR-IGG), Via Gradenigo, 6, 35131 Padova, Italy

ARTICLE INFO

This manuscript was handled by Emmanouil Anagnostou, Editor-in-Chief

Keywords:
Sediment transport
Venice Lagoon
Flood barriers
MoSE project
In-situ instrumental network
Storm surge

ABSTRACT

This study investigates the effects of flow regulation by the floodgate system (MoSE: Electromechanical Experimental Module) on sediment and water exchanges between the Venice Lagoon and the Adriatic Sea, during two significant storm surges in 2022 and 2023. An integrated observation system, which combines satellite-derived products and data from in-situ instrumental networks, was implemented at the three lagoon inlets (Lido, Malamocco and Chioggia). The high spatial and temporal resolution of continuous in-situ data allowed to characterize the complex interactions between sediment fluxes driven by tidal flow and the repeated and prolonged activations of the floodgates, considering the intense particle resuspension within the lagoon and along the coasts by wind waves. Our findings reveal a quite similar net sediment loss from the lagoon during each event (~13,880 tons and ~ 14,850 tons), but with distinct spatial and temporal patterns in the four inlet channels. During the 2022 event, sediment export during ebb tides exceeded import during floods, leading to a net loss at all inlets (Chioggia ~ 4,720 tons, Malamocco ~ 3,360 tons, Lido ~ 5,800 tons). By contrast, in the 2023 event, sediment import dominated in the northern basin (Lido ~ 5,900 tons), while export prevailed in the central and southern basins (Malamocco ~ 6,570 tons, Chioggia ~ 14,160 tons). As observable in satellite images, this input at north is related to fine particles resuspended under northeasterly wind along the adjacent coast and transported in the lagoon by flood tidal currents. The presence of jetties at the inlets interrupts the natural coastal drift at south inhibiting such inputs at central and southern basins. Besides being effective in preventing high waters in Venice, this study suggests that the regulation operated by the barriers can potentially determine positive or negative short-term feedbacks on the lagoon sedimentary budget, minimizing sediment losses from the lagoon or blocking the inputs from the nearby coast. In an operational context, near real-time information deriving from the tested methodology can support an effective management of the MoSE system, adaptable to the evolution of meteo-marine conditions. In the long term, adaptive strategies are essential to prevent alterations of the sediment fluxes and the consequent loss of habitat in shallow tidal environments that are already threatened by natural and anthropogenic pressures.

1. Introduction

About 32,000 lagoons are reported along 13 % of the world's coastline (Carter and Woodroffe, 1994) and they represent complex ecosystems highly sensitive to environmental variability and anthropogenic pressures (Ferrarin et al., 2014; Newton et al., 2014) and to the impact of climate change. Coastal lagoons are dynamic environments located at the interface of land and sea and they are vital for biodiversity, coastal protection, and human livelihoods. Their vulnerability underscores the urgent need for effective management strategies and several approaches were adopted in coastal lagoons, to mitigate the impacts of sea level rise, including the construction of infrastructures such as dikes and barriers to regulate water flow and reduce the risk of inundation (Gibbons and Nicholls, 2006; Cooper and Lemckert, 2012; Mahdian et al., 2023). Significant examples of such interventions are found worldwide. For example, in the Ria Formosa lagoon system along

* Corresponding author.
E-mail address: gianmarco.scarpa@cnr.it (G.M. Scarpa).
[1] Both authors contributed equally to this work.

https://doi.org/10.1016/j.jhydrol.2024.132588
Received 6 October 2024; Received in revised form 4 December 2024; Accepted 5 December 2024
Available online 24 December 2024

the southern coast of Portugal a series of artificial inlets and culverts were constructed to modulate the tidal flow, aiming to preserve the ecological integrity and sustain traditional fishing practices (Kombiadou et al., 2019; Newton et al., 2022). Similarly, in the Coorong coastal lagoon, Australia, systems of barrages and weirs were implemented to regulate water levels and salinity gradients (Webster 2011). In the Chesapeake Bay, United States, an extensive series of artificial channels and dykes was built to control nutrient runoff and sedimentation, mitigating the impacts of eutrophication and shoreline erosion (Russ and Palinkas, 2020; NOE et al, 2020). A long-awaited and discussed intervention is the system of mobile barriers built at the inlets of the Venice Lagoon, Italy. Known as MoSE, the Italian acronym for Experimental Electromechanical Module, the infrastructure already defends Venice from flooding by lifting a total of 78 movable gates, normally housed on the seabed, on a forecast of a high tide in the northern Adriatic Sea (Zarotti, 2022; Umgiesser, 2020). Since October 2020, the MoSE system has operated in a preliminary experimental mode and the inlets were already closed 84 times until May 2024. The frequency and duration of closures are expected to increase in view of the ongoing processes and predicted scenarios of relative sea level rise (RSLR) and climate change (Mel, 2021; Tagliapietra and Umgiesser, 2023) with several implications for hydrodynamics (Ferrarin et al., 2010), wind waves (Favaretto et al., 2022), lagoon water temperature (Ferrarin et al., 2024), fluxes of sediments, contaminants and organisms (Ferrarin et al., 2015) and morphodynamics of saltmarshes (Tognin et al., 2021). Although the MoSE system is proving to be an efficient and essential measure for the physical safeguard of Venice and its unique cultural heritage from high waters (Giupponi et al., 2024), the first effects of its operation on the efficiency of fisheries and port activities and on the preservation of ecosystem services have already been ascertained. The effects of the altered hydrodynamics induced by the operational phase of the MoSE system were observed by Leoni et al. (2022) that demonstrated how the dissolved oxygen balance in the water column is affected by the increase in water residence time. Also, Baldassarre et al. (2023) investigated the effects of the MoSE-related alterations on the microphytobenthic community. Tognin et al. (2021) proved that the reduction of salt marsh inundation, related to the MoSE operations, critically influences their resilience to RSLR by reducing inorganic deposition during storm-surge events which, though episodic, contribute to marsh vertical accretion. Moreover, the artificial reduction of water levels inside the lagoon during the MoSE operations might enhance wave-induced sediment resuspension from the lagoon beds, promoting in-channel deposition and/or flushing-out of sediments, through the channel network and eventually the inlets (Tognin et al., 2022).

For a realistic assessment of the impacts of lagoon closures on sediment dynamics, the in-situ monitoring of water and particle exchanges becomes crucial, especially during storm events when large amounts of materials are mobilized by wind waves and normally transported through the inlets. In this context, the existing information mostly dates back to the period before the construction of the barrier system. Experimental measurements of solid transport based on the use of Acoustic Doppler Current Profilers (ADCPs) started from 2004, (Defendi et al., 2010) and continued in the following decade until 2019, mostly to monitor the impacts of the construction works on the lagoon ecosystem.

To cover the data gap for the assessment of alterations in the lagoon-sea exchanges, an observation system integrating satellite images, in-situ water parameters and hydrodynamic measurements was implemented concomitant to the pre-operative experimental phases of the MoSE floodgates. The instrumental network continuously monitor the fluxes of water and sediments through the Lido inlet of the Venice Lagoon (Scarpa et al., 2022).

Here, we analyze data from the integrated observation system, now extended to the three inlets, to investigate the overall lagoon-sea exchanges and short-to-long-term variations on sediment transport pathways in this phase of experimental operativity of the MoSE floodgates. We focus on two storm events with a prolonged activation of the MoSE barriers to investigate the evolution of sediment transport within a time-window of one week (November 2022 and January 2023). The sediment budget for the Venice Lagoon inlets is also estimated on the same time-intervals to assess the impact of the barrier activation in extreme tide and weather conditions.

2. Study site

The Venice Lagoon is located in the northern Adriatic Sea (NAS) and extends over an area of about 550 km^2. It is connected to the Adriatic Sea through three inlets: Chioggia (CH), Malamocco (MAL) and Lido (Fig. 1). The inlets are from 450 to 900 m wide and are up to 20 m deep. An artificial island splits the Lido inlet into two distinct branches, Treporti (TRP) and S. Nicolò (SN) resulting in a total of four inlet channels. A semidiurnal tide with a range of about 1 m induces a total water exchange per cycle of the order of 10,000 m^3/s, reaching 20,000 m^3/s during spring tides (Gačić et al., 2002).

Extreme high tides occur periodically in the NAS as a combination of atmospheric forcing, astronomical tide and free oscillations (Lionello et al., 2021). They represent the main threat to coastal areas by causing a range of potential hazards, such as inundation and coastal erosion, as well as damages to the vulnerable artistic and cultural heritage of Venice (Ferrarin et al., 2022). Storm surges, which often produce the largest contribution to the floods, are generally triggered by a south-easterly wind, called Sirocco, which is mainly produced by cyclones with pressure minimum centered on the north-western Mediterranean Sea, combined with the NAS bathymetry and coastal orography (Lionello, 2005; Lionello, 2012). Another wind configuration causing storm surges is a combination of strong north-easterly wind, locally called Bora, over the NAS and Sirocco over the southern Adriatic. Free oscillations of the water surface, known as seiches, with periods determined by the normal modes of the Adriatic Sea basin, can continue to cause flooding in the Venice Lagoon for several days after the passage of the storm (Bajo et al., 2019; Ferrarin et al., 2021). High tides from the NAS propagate into the Venice Lagoon through the four inlet channels and along the tidal channels, expanding laterally into the wetlands. A wind setup, which may exceed 50 cm, on the water level between the southern and the northern parts of the lagoon can be produced by strong Bora and Sirocco winds (Mel et al., 2019). To prevent widespread flooding of the city of Venice, the MoSE system is currently activated when the forecasted level of the NAS is greater than 110 cm above the local datum at Punta Salute (PS), closing in advance at an initial level of 70 cm inside the lagoon.

3. Materials and methods

This study was based on the integration of instrumental networks deployed at the four inlet channels of the Venice Lagoon, appropriately calibrated through extensive in-situ measurement campaigns and data processing, for the assessment of water and suspended sediment exchanges with the NAS during selected and representative periods of multiple activations of the MoSE system. A schematic procedure of the data processing operations is presented as a flowchart in the Supplementary Materials (Supplementary 1).

3.1. In-situ network

Continuous in-situ turbidity measurements (T_{OBS}), expressed in Formazin Nephelometric Units (FNU), were made using OBS-501 turbimeters (Campbell Scientific, Loughborough, UK), installed on steel structures adjacent to the channels on the concrete lateral structures of the MoSE system (blue dots in Fig. 1). T_{OBS} was measured at a depth of 2 m by detecting the intensity of light scattered from suspended particles in the water with an acquisition frequency of 5 min. An anti-fouling system prevented data drift related to lens darkening or opacification.

At the bottom of each inlet channel (red dots in Fig. 1), an ADCP (600

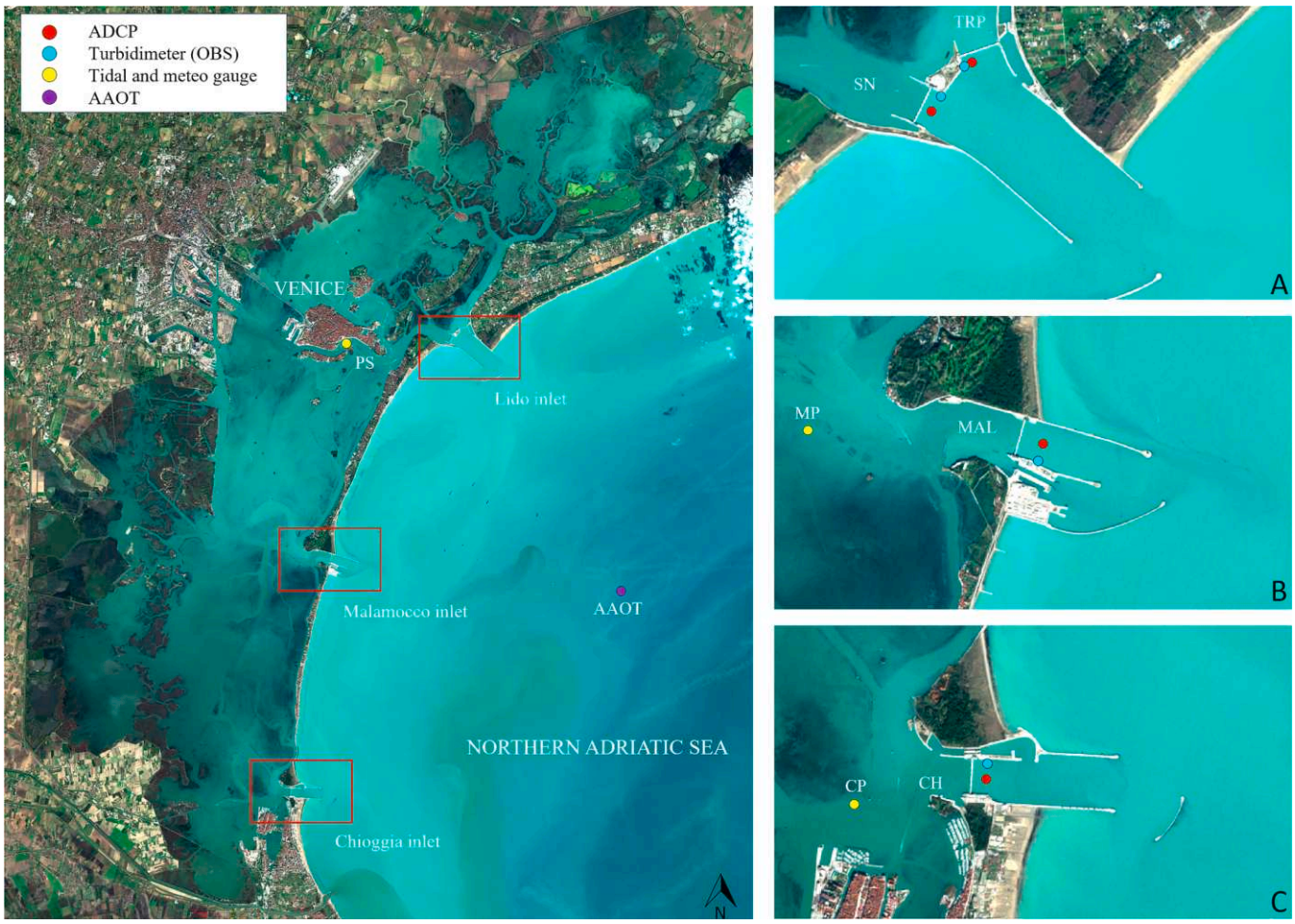

Fig. 1. Copernicus Sentinel-2 true-colour composite of the Venice Lagoon (24th November 2022), acquired when the MoSE floodgates, normally housed on the seabed, are operating. (A) Lido inlet, divided into the SN (400 m wide, 12 m deep, 20 gates) and the TRP channels (420 m wide, 6 m deep, 21 gates); (B) MAL inlet (380 m wide, 14 m deep, 19 gates); (C) CH inlet (360 m wide, 12 m deep, 18 gates). The locations of the instrumental network and monitoring stations, used in this study, are also indicated: bottom-mounted upward looking ADCPs (red dots); CP, MP and PS tidal and meteo gauge stations (yellow dots); OBS turbidimeters (blue dots); Acqua Alta Oceanographic Tower (AAOT) (purple dot). (For interpretation of the references to color in this figure legend, the reader is referred to the web version of this article.)

KHz RDI Workhorse Monitor ADCP; Teledyne RD Instruments, San Diego, CA, USA) was deployed upward-looking for continuous measurement of current velocity and direction and acoustic backscatter along the water column with a sampling interval of 5 min and a 0.5 m vertical cell size. The monitoring platform was installed and is managed by the Consorzio Venezia Nuova (the concessionary of the Authority for the implementation of measures to safeguard Venice and its lagoon) to monitor the flow in the inlets during the operations of the barriers. The instruments are located on a sandy bottom immediately seaward of the MoSE structures, approximately at the center of the channel cross-section whose margins are delimited by the jetties. It should be noted that in the case of the TRP inlet channel the position of the ADCP profiler is not exactly at the center of the section.

Tidal levels for the three sub-basins of the lagoon were obtained from time series recorded by the Punta della Salute (PS), Malamocco Porto (MP) and Chioggia Porto (CP) tide gauge stations managed by the Municipality of Venice (yellow dots in Fig. 1). Wind direction and velocity were recorded every five minutes at the AAOT at 18 m above the sea surface (purple dot in Fig. 1).

3.2. In-Field activities

Two different types of in-situ measurements were conducted for the estimation of Suspended Sediment Concentration from turbidity records (SSC_{OBS}) and to derive time series of water discharge from ADCP (Q_{ADCP}).

To convert T_{OBS} into SSC_{OBS} (mg L^{-1}), a site-specific calibration curve of the two variables was empirically derived for each station (Minella et al., 2008). Water samples were collected under different meteo-marine conditions at the same depth and within 1 m of the instruments, synchronized with turbidity measurements. SSC was determined by filtering the samples through 0.4 μm polycarbonate filters, followed by drying at 105 °C and weighing.

The vertically averaged flow velocity (v_{av}), measured by the fixed ADCPs at the bottom of the 4 inlet channels, was linearly related to direct discharge measurements performed with a boat-mounted downward looking ADCP (600 kHz RDI Workhorse Rio Grande, Teledyne RD Instruments, San Diego, CA, USA) along transects perpendicular to the flow. For this purpose, a large series of transects were acquired in different meteo-marine and tidal conditions at the 4 inlet channels obtaining a total number of more than 400 match-ups of velocity and discharge data. Time series of instantaneous discharge Q_{ADCP} were then calculated from the records of v_{av} using the obtained regression equations, according to the index-velocity method described by Simpson and Bland (2000).

3.3. Data processing

For the conversion of the acoustic backscatter intensity (I_{ADCP}) measured by bottom-mounted ADCPs along the water column into profiles of SSC_{ADCP}, we used SSC_{OBS} time series obtained from the fixed turbidimeter stations at 2 m depth, as input data for the ViSea Data Acquisition Software (ViSea DAS; Aqua Vision) and its Plume Detection Toolbox (PDT) package, based on the method described by Deines (1999) and updated in Mullison (2017). To obtain a reliable parametrization of each ADCP at the 4 inlets, the procedure was applied on time-windows of 20 days (from November 10th to November 30th, 2022, and from January 10th to January 30th, 2023), which included the two storm surge events of interest. The considerably large amount of SSC_{OBS} data for the processing (about 5000 match-ups) permitted to improve the representativity of acoustic backscatter conversion compared to the use of SSC from single water samples. The conversion procedure of ViSea DAS was integrated with a statistical analysis, known as robust regression, that permitted to identify and remove outliers due to instrumental and ambient transient anomalies, improving the overall model fit. Additional input parameters were: i) temperature and salinity profiles for determining acoustic properties of the water; ii) median grain size of suspended particles (25–30 μm), determined with LISST-100X (Sequoia Scientific Inc., 2004).

Starting from the bidimensional matrix of backscatter along the vertical profile above the bottom-mounted ADCP, the time series of SSC_{ADCP} along the water column and its vertically averaged particle concentration SSC_{AVG} were calculated. Due to the limitations of ADCPs, only I_{ADCP} and SSC_{ADCP} data from the water column directly above the instrument were considered, excluding the surface (about 1.0 m) and the near-bed zone (about 2.0 m). Time series of instantaneous values of solid flux (in kg s^{-1}) for each inlet were then computed by combining the Q_{ADCP} and the SSC_{AVG} from the four bottom-mounted ADCPs (Defendi et al., 2010), assuming that this is representative of the SSC distribution in the channel cross section. The assumption is justified by the good correspondence between SSC_{AVG} and the average particle concentration in the channel cross section determined from the backscatter of the boat-mounted ADCP transects. The only exception is the markedly asymmetric distribution of SSC in the channel section of TRP during strong northeasterly winds (Defendi et al., 2010; Scarpa et al., 2022). Considering that the fixed ADCP is located on the center-south side of the TRP inlet section, an underestimation of the SSC and sediment flux may occur in these specific conditions. To investigate the sediment exchanges within the study periods, the time series of solid flux were integrated on a 5-minute interval and plotted as cumulative values of suspended sediment load (SSL) for the four inlet channels.

3.4. Remote sensing data

Sentinel-2 (S2) satellite images (Level-1C), processed by the European Space Agency (ESA) under the European Union Copernicus Programme, were downloaded from the Copernicus Browser (https://browser.dataspace.copernicus.eu). For the periods of interest, only two cloud-free S2 images were available: November 24th, 2022, and January 25th, 2023. Pseudo true-color composites and satellite-derived turbidity (T_{SAT}) maps at a 10-meter resolution were generated from the S2 data, following the methodology described in Braga et al. (2020) and Braga et al. (2022). In brief, the S2 images were radiometrically calibrated and atmospherically corrected using ACOLITE [Version 20231023.0], with the dark spectrum function approach (Vanhellemont and Ruddick, 2018; Vanhellemont, 2019). Pseudo true-color composites were created from ACOLITE-derived water-leaving reflectance at 665, 560, and 492 nm. Additionally, T_{SAT} maps, expressed in formazin nephelometric units (FNU), were obtained according to Dogliotti et al. (2015).

4. Results and discussion

4.1. In-situ data and derived variables

From February 2020 to November 2023, a total of 112 water samples were analyzed for the site-specific conversion of T_{OBS} into SSC_{OBS}. Because of the longer deployment of the instruments, a larger number of samples were collected at TRP and SN stations compared to MAL and CH. The plots in Fig. 2 show the correlations between T_{OBS} and SSC (mg L^{-1}) obtained for each inlet channel.

The highest SSC were found at TRP, with a range of 1 to more than 90 mg L^{-1}. At SN and MAL, the ranges were lower (1–60 mg L^{-1}), while at CH, in-situ SSC did not exceed 40 mg L^{-1}. A robust correlation is observable across the entire sampled ranges, with a coefficient of determination (R^2) higher than 0.95 for the 4 inlet channels. The resulting regression equations were used to convert T_{OBS} data of each station into SSC_{OBS}.

Similarly to what demonstrated for SN and TRP (Scarpa et al., 2022), the correlations between instantaneous discharge data obtained from ADCP transects and v_{av} measured by fixed ADCPs (the index-velocity) at MAL and CH are significant with coefficients of determination (R^2) close to unity (Fig. 3). These results confirm that the index velocity can be used as a reliable proxy of discharge in all the investigated sections also thanks to the fixed geometry of the channel section that is artificially maintained only allowing negligible changes. The regression equations of Fig. 3 were then used to calculate time series of instantaneous discharge starting from v_{av} obtained from ADCP datasets.

In Fig. 4 we present the scatterplots of the acoustic backscatter versus SSC_{OBS}, for the fixed ADCPs at the four inlet channels for the two periods selected for this analysis. The number of match-ups varied according to the amount of validated data in each time series, providing a site-specific and instrument-specific relationship over a wide range of concentrations. The differences observed between the two periods were due to service activities like repositioning and/or replacement of the ADCPs. The slope and offset derived from the robust regression in each scatterplot were used in ViSea DAS to convert time series of I_{ADCP} into the corresponding SSC_{ADCP}. To estimate the measurement uncertainty of the SSC derived from ADCP backscatter conversion (SSC_{ADCP}), we compared the SSC values estimated using the regression curves (red lines in Fig. 4) with the SSC_{OBS} values derived from turbidity data. This comparison, presented in the supplementary material (Supplementary 2) provided a Mean Absolute Error (MAE) for each period and each inlet ranging from 5.52 mg L^{-1} to 12.8 mg L^{-1}. The lowest MAE values for both 2022 and 2023 were observed at SN (5.52 mg L^{-1} in 2022 and 5.59 mg L^{-1} in 2023), while the highest values were consistently recorded at TRP, with 8.94 mg L^{-1} in 2022 and 13.81 mg L^{-1} in 2023.

As described in the methods section, time series of instantaneous solid flux for each inlet channels were then computed for the periods of interest by combining the Q_{ADCP} and the SSC_{AVG} from the four bottom-mounted ADCPs and used for the estimation of SSL.

4.2. Meteo-marine conditions

Figs. 5 and 6 show the meteo-marine conditions for November 21st−27th 2022 and January 19th − 25th 2023, respectively: the hourly fields of the horizontal wind speed at 10 m height (U10) in the Adriatic Sea, derived from the ECMWF ERA5 reanalysis (available from the Copernicus Climate Data Store; (Hersbach et al., 2020) (panel A), the time series of wind speed and direction measured at AAOT (panel B) and the tide levels measured within the Venice Lagoon at the three gauge stations (PS, MP and CP) and at AAOT (panel C). These events were characterized by different meteorological conditions and are of particular interest for the purposes of this study because in both cases, the forecasted tidal level at PS required a prolonged activation of the MoSE barriers with multiple closures of the floodgates and partial openings of single inlets.

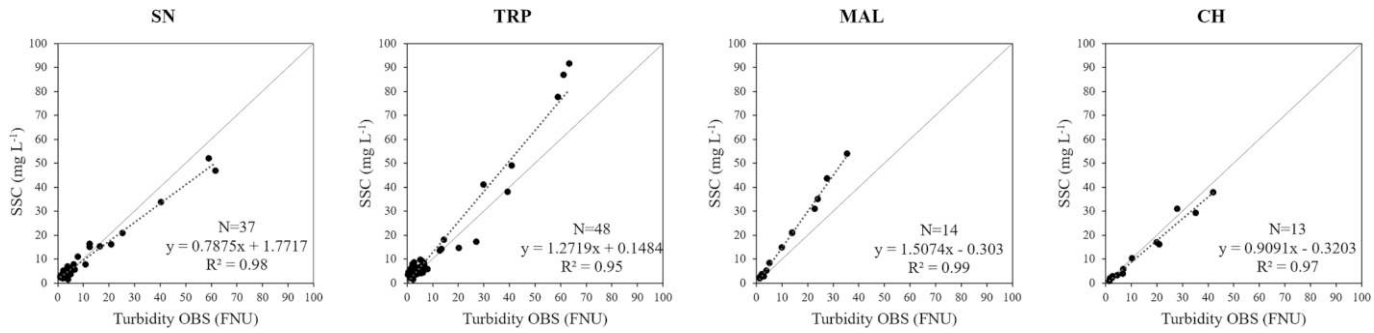

Fig. 2. Scatter plot of the turbidity data retrieved from the fixed turbidimeters (T_{OBS}) and suspended sediment concentration (SSC) derived from water samples, for the stations SN, TRP, MAL and CH. The linear regression equations and the coefficients of determination (R^2) are reported in the plots; red dotted lines are the best-fit regression; the grey solid line is the 1:1 line. (For interpretation of the references to color in this figure legend, the reader is referred to the web version of this article.)

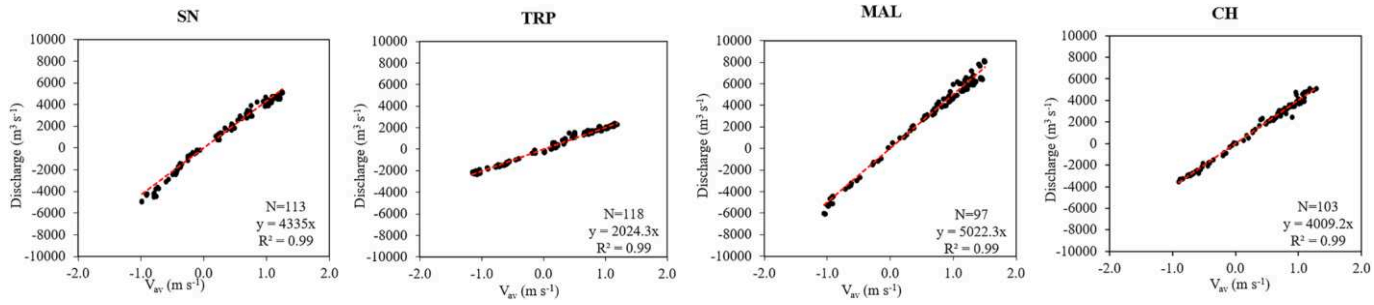

Fig. 3. Linear regressions between the vertically averaged velocities (v_{av}) by fixed ADCPs (the index-velocity) and instantaneous discharge data from the ADCP transects for SN, TRP, MAL and CH stations. Red dashed lines are the best-fit regression. Scatterplots of SN and TRP are (For interpretation of the references to color in this figure legend, the reader is referred to the web version of this article.)
adapted from Scarpa et al. (2022).

As described by Mel et al. (2023), between November 21st and 22nd 2022, the large-scale weather conditions in the eastern Atlantic and Mediterranean regions triggered the ideal configurations for storm surges in the Adriatic Sea, that normally cause the occurrence of the highest tides along the Venice coastlands (Cavaleri et al., 2019). From the evening of the November 21st until the night of the 22nd, a strong southeasterly wind (Sirocco) prevailed in the Adriatic Sea, coupled with an intense easterly to northeasterly wind pattern over the northern basin, reaching maximum gusts of 28 m/s from NE at AAOT (Fig. 5A and B). These meteorological conditions generated an extreme storm surge event with maximum sea levels of 1.73 m at AAOT and more than 2 m at stations located on the coast at 8:35 (UTC) of the 22nd. A first partial MoSE operation in the afternoon of the November 21st involved only the TRP and SN inlet channels, while CH and MAL remained open. The closure of Lido inlet allowed the modulation of the level within the northern basin of the lagoon (the city of Venice), determining a slower flood phase and a maximum level of 0.78 m at PS, while the tidal peak reached 0.98 m at 20:15 at AAOT. At MP and CP gauge stations, where the inlets remained open, the trend of the tide was more similar to the one of AAOT with peaks of 0.86 m at 21:10 in MP and 0.93 at 20:35 in CP. Considering the tidal forecast, the MoSE floodgates were then raised at 1:15 of 22nd in all the inlets, isolating the lagoon from the sea and limiting the internal tidal levels to less than 0.75 m for the first 6 h (Fig. 5C). With the intensification of northeasterly winds, which blew along the main axis of the lagoon, the water level at CP station started to increase up to 1.10 m due to the wind setup, while a decrease was observed at PS (about 0.50 m), with an average difference in the maximum observed water levels between the two stations equal to 0.60 m. To prevent the flooding of the southern lagoon, while keeping close the other inlets, the barriers of CH inlet were then temporarily opened for an interval of 5 h during the ebb tide phase, favoring a rapid drop of water level. In non-regulated conditions, this Bora wind setup would induce a net southward residual current affecting the flow rate across the inlets, with a prevailing inflow from Lido and outflow from Chioggia, which would result in a reduction of the internal north–south gradient of sea level (Mel et al., 2019). The overall operation of MoSE barriers in this initial phase of the event covered a period of about 20 h. In the following three days, despite a decrease of wind speed below 5 m s^{-1}, the seiches in the Adriatic basin induced three consecutive high tides. At AAOT, sea levels reached 1.42 m at 8:15 of 23rd, 1.34 m at 8:00 of 24th, and 1.14 m at 9:20 of 25th, while the water level in the lagoon was maintained below 0.80 m thanks to the activation of the MoSE barriers in three other intervals (gray boxes evidenced in Fig. 5C).

On January 20th and 21st, 2023, synoptic meteorological conditions led to the development of a strong depression system with a very deep baric minimum over the Adriatic Sea, accompanied by strong Sirocco winds over southern Adriatic, with a consequent rise of sea levels over the entire basin, and intense Bora winds over the northern and center Adriatic. In the NAS, northeasterly winds persisted for the whole study period (January 19- 25th, 2023) with speed mainly above 10 m/s, reaching two maximum values of 22 m/s and 24.2 m/s, respectively at 22:45 of the 22nd and at 8:05 of the 23rd at AAOT (Fig. 6). These conditions generated an intense storm surge event with maximum sea level of 1.35 m at AAOT at 09:35 of the 23rd. Considering the tidal forecast, the MoSE floodgates were raised from 5:00 of the 21st in all the inlets, blocking the input from the sea and maintaining the internal water levels to less than 0.75 m (Fig. 6C). In the following days, the strong steady wind conditions induced four consecutive high tides. At AAOT, sea levels reached 1.14 m at 8:45, 0.94 m at 22:55 of 22nd, 1.35 m at 08:15 and 0.89 m at 22:15 of 23rd, while the water level in the lagoon was limited below 0.80 m thanks to the activation of the MoSE barriers (gray boxes evidenced in Fig. 6C). During the fourth closure, which lasted 9 h, an internal wind setup determined a difference between CP and PS of 0.29 m.

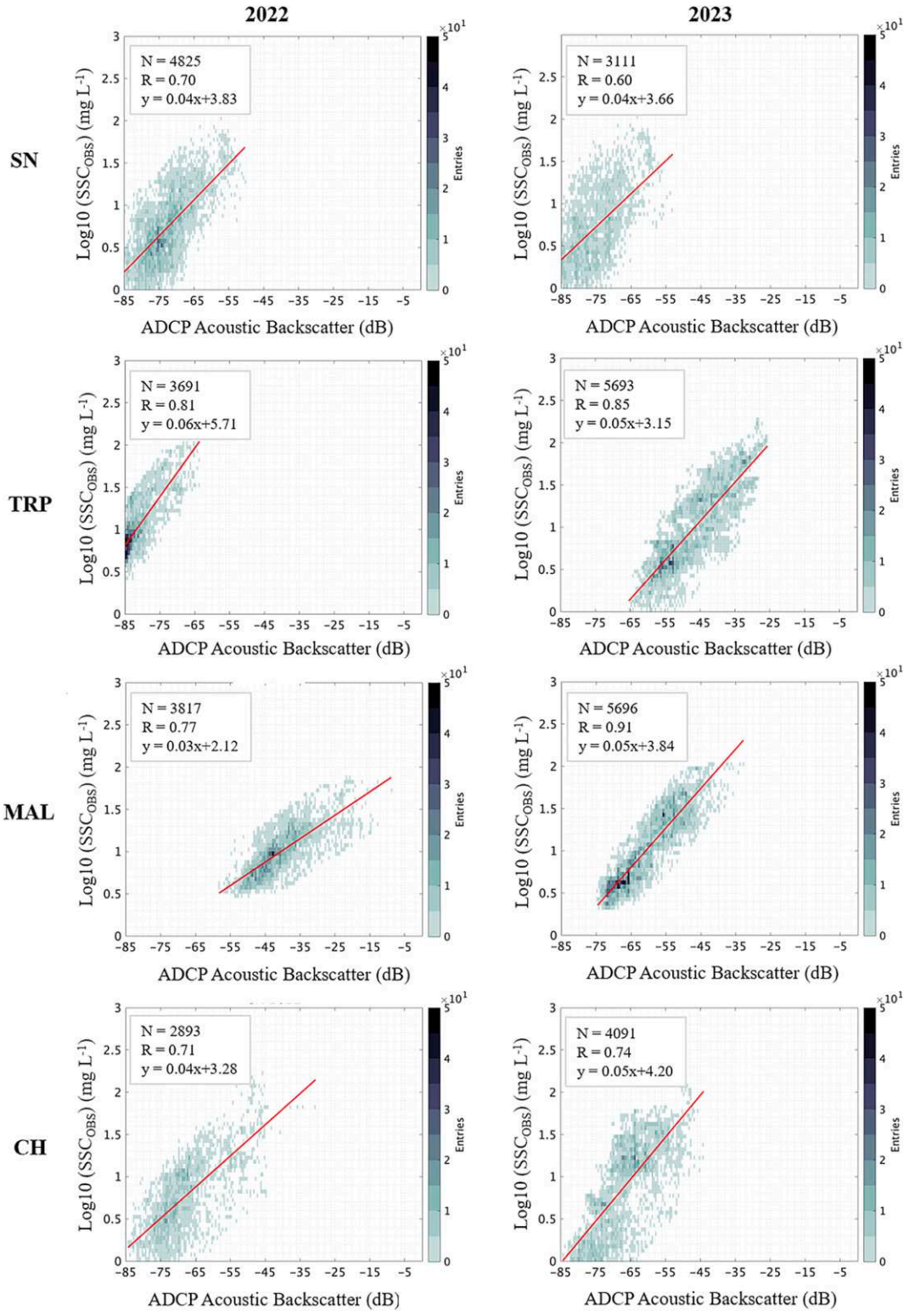

Fig. 4. Calibration of the acoustic backscatter of the bottom-mounted ADCPs for the two studied periods. Linear regressions between bottom-mounted ADCPs backscatter and Log10 of SSC_{OBS} .

4.3. Hydrodynamics and suspended sediment distribution

In Figs. 7 and 8, the time series of the channel-axis component of current speed (panel A) and suspended sediment concentration along the water column (panel B) for the four inlet channels, derived from the bottom mounted ADCPs (SSC_{ADCP}), are presented. Moreover, v_{av} and T_{OBS} are plotted with white lines, overlaid to panel A and panel B, respectively, to support the interpretation of the events. Negative velocities indicate flood tidal currents, while positive velocities indicate ebb tidal currents.

In the event of November 2022, the five activations of MoSE barriers are highlighted by red boxes in Fig. 7. Data clearly show the

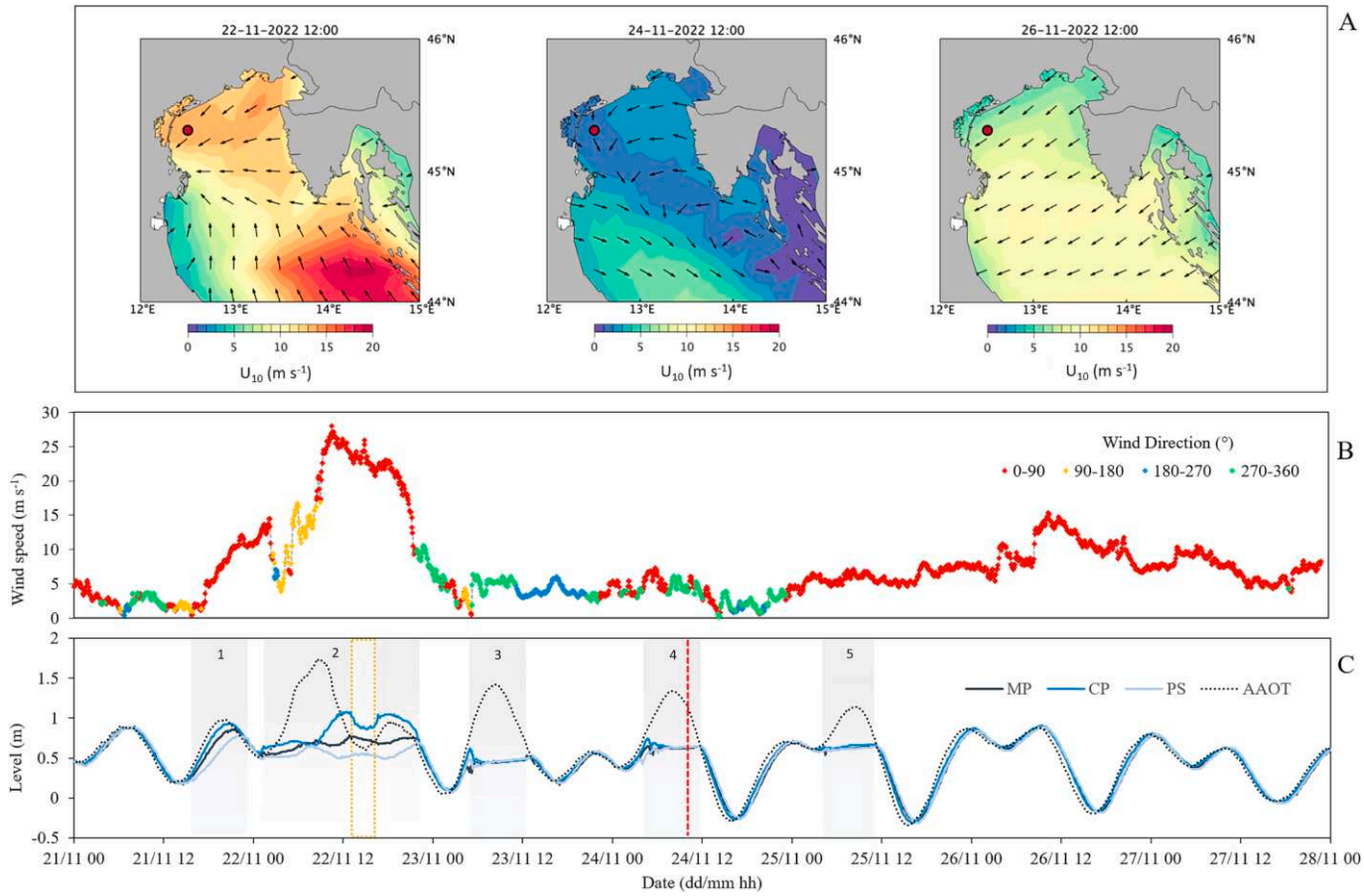

Fig. 5. Meteo-marine conditions for the studied event from November 21st to 27th 2022. Panel A: surface wind speed at 10 m height (U10) and direction fields from ERA5 atmospheric reanalysis for November 22nd, 24th and 26th 2022 at 12:00 UTC. The red dot in the maps of this panel indicates the location of the Acqua Alta Oceanographic Tower (AAOT). Panel B: time series of wind direction and speed measured at AAOT (red = 0°–90°, yellow = 90°–180°, cyan = 180°–270°, green = 270°–360°). Panel C: water level measured at PS, MP, CP and AAOT. Areas with gray background indicate the MoSE. closure intervals. The orange dotted box identifies the partial opening of the CH inlet. The vertical dashed red line marks the S2 satellite overpass time. (For interpretation of the references to color in this figure legend, the reader is referred to the web version of this article.)

hydrodynamic effects of the closure (Fig. 7A), as current velocities dropped to zero, except TRP where a slight negative residual current is observed ($v_{av} \sim -0.2$ m/s). Generally, SSC_{ADCP} also reduced considerably during the closures, because of the interruption of sea-lagoon exchanges at the inlets, except for a sudden increase in the initial phases of the closures that is particularly evident at the start of the closure 2 in MAL and CH and correspond to instantaneous pulses of v_{av} (Fig. 7). This increase is attributed to the turbulence locally generated by the movement of the gates as they are raised into position and is occasionally detected by the instruments in relation to the sequence of maneuvers that could change in the different operations. Typically, on a given inlet the array of floodgates is raised on a time interval of about 30 min (Umgiesser, 2020) and the individual gates are moved in an alternate sequence, as visible in publicly available videos that also document the temporary turbulence and turbidity generated in the initial phases of the gate movement: (https://www.youtube.com/watch?v=acI8Otju5hI, https://www.youtube.com/watch?v=MFrZLbjlrRY). It should be noted that the MoSE system is still in its experimental phase, and operational protocols are still under development and details of the closing procedure are given internal reports of the Authority for the implementation of measures to safeguard Venice and its lagoon.

During the first partial closure (box 1 in Fig. 7 panels A and B), the water velocities were close to zero in SN and TRP, while they reached maximum values of 1.65 m/s and 0.85 m/s at MAL and CH, respectively. Similarly, the estimated SSC_{ADCP} at TRP and SN were also close to zero, while they reached maximum values of 84 mg L^{-1} and 17.4 mg L^{-1} at MAL and CH, respectively.

From 1:15 of 22nd, the MoSE floodgates were raised in all the inlets, and the lagoon remained partially closed for about 23 h (box 2 in Fig. 7 panels A and B). In correspondence of the maximum wind speed, an increase in SSC_{ADCP} was recorded in the water column with higher values at the surface. This can be related to a combination of factors, such as: weak residual flow driven by leakages, through the unsealed joints of the gates, and seawater accumulation inside the inlet channels, both carrying sediment resuspended by wind waves on the nearby shores (https://earthobservatory.nasa.gov/images/149151/venice-holds-back-the-adriatic-sea). T_{OBS} at TRP reached values of 100 FNU, probably due to the resuspension of fine sand from the bottom of the northern side of the inlet channel that is relatively shallow (about 3 m) and may be exposed to Bora waves and their diffracted components. The temporary opening of the CH inlet from 12:55 to 17:05 determined a net seaward flow in the inlet with a maximum value of current velocity of 0.95 m/s at 13:55 (Fig. 7A) and an increase in SSC_{ADCP} along the water column, that reached 55 mg L^{-1}. This is also evident from the T_{OBS} measurements, where a peak of 144 FNU was recorded at 14:40. (Fig. 7B). This material was likely originated from the intense resuspension by wind waves on the tidal flats of the southern lagoon basin. A more detailed figure for the period between November 21, 2022, and November 23, 2022, is available in the supplementary materials (Supplementary 3).

Following the complete opening of the inlets at 21:40 on November 22nd, a sudden pulse in the seaward flow velocity occurred (Fig. 7A)

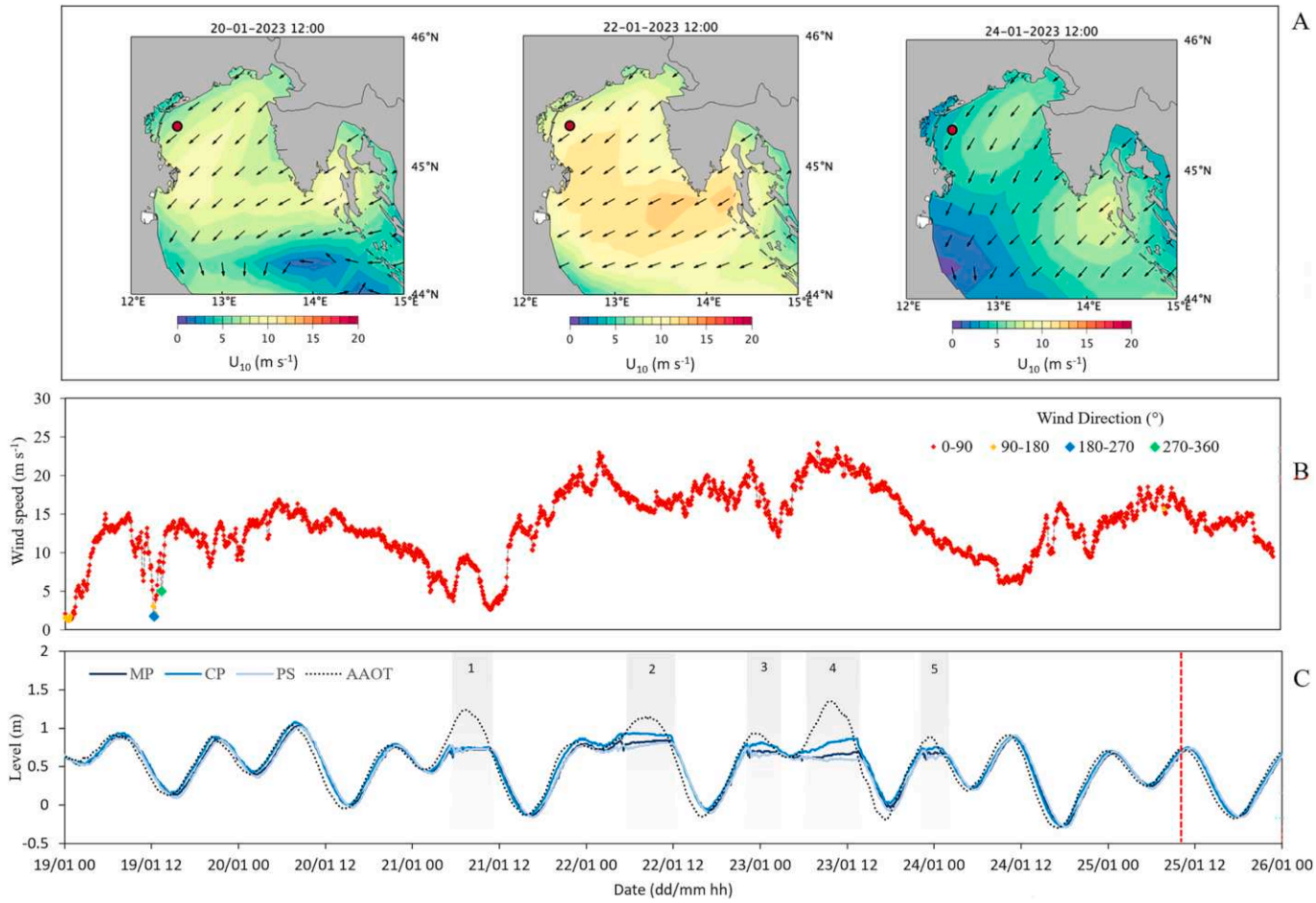

Fig. 6. Meteo-marine condition for the studied event from January 19th to 26th 2023. Panel A: surface wind speed at 10 m height (U10) and direction fields from ERA5 atmospheric reanalysis for January 20th and 24th at 12:00 UTC. The red dot in the maps of this panel indicates the location of the Acqua Alta Oceanographic Tower (AAOT). Panel B: time series of wind direction and speed measured at AAOT (red = 0°–90°, yellow = 90°–180°, cyan = 180°–270°, green = 270°–360°). Panel C: water level measured at PS, MP, CP and AAOT. Areas with gray background indicate the MoSE closures intervals. Vertical dashed red line marks the S2 satellite overpass time. (For interpretation of the references to color in this figure legend, the reader is referred to the web version of this article.)

with a progressive increase in T_{OBS} and SSC_{ADCP}, that exceeded 100 mg L^{-1} in the lower layer of water column at TRP (Fig. 7B). This process can occur at every opening of the inlets upon the activation of the tidal flow. Similarly to what described for the temporary opening at CH, the higher SSC_{ADCP} was due to suspended material mobilized by strong winds in the internal lagoon areas and transported through the channel network and the inlets to the open sea by the ebb tidal flow. As proved by Tognin et al. (2022), reduced water levels due to the closure can further increase bottom shear stress, exacerbating sediment resuspension in the inter-tidal and subtidal zones, generalized sediment transport and in-channel deposition. The temporary sediment accumulation in the channel seabed can be easily mobilized by the intense current velocities induced by the strong hydraulic gradients generated by the opening of the floodgates. This is quite evident after the 4th and 5th closure, that occurred in relatively calm wind conditions but gave rise to a high export of suspended sediments, particularly for the TRP which drains the large extents of tidal flats and salt-marshes of the northern lagoon.

In the investigated period of January 19th−26th, 2023, the storm-surge barrier system was raised five times, simultaneously at all the inlets (red boxes in Fig. 8A and B), while intense Bora wind (over 10 m/s) prevailed for almost the entire period considered. Compared to the previous case of November 2022, the estimated SSC_{ADCP} after the opening of the inlets was higher throughout the period for all the inlets, with maximum values along the water column exceeding 150 mg L^{-1} at SN and TRP. The highest SSC_{ADCP} generally corresponded to the ebb tidal flow at MAL and CH stations and to flood tide at SN, while the trend of SSC_{ADCP} at TRP was slightly symmetric during ebb and flood phases. This suggests a relevant inward transport of suspended sediments from the adjacent Adriatic coasts into the Lido inlet under Bora wind, as described by Scarpa et al. (2022). This is particularly evident after the second opening on January 22nd at SN, when maximum incoming flow velocity and maximum SSC_{ADCP} reached 1.35 m/s and 151 mg L^{-1} at 21:20, respectively. A similar condition was observed the following day, January 23rd, at 20:15, with flow velocity at 1.43 m/s and maximum SSC_{ADCP} at 199 mg L^{-1}. Analogous behavior characterized TRP during these intervals, with inflow water velocity of 1.4 m/s and concentrations of 118 mg L^{-1}, and 1.25 m/s and 94 mg L^{-1} during the subsequent flood tide peak. A more detailed figure for the period between January 22, 2023, and January 24, 2023, is available in the supplementary materials (Supplementary 4). The trends of T_{OBS} were quite similar to SSC_{ADCP}. However, it should be noted that at TRP the T_{OBS} reached extremely high values during the flood tide on 23rd (about 250 FNU). These pulses of suspended sediments derived from the fine materials resuspended under Bora wind along the northern coast of the Adriatic Sea and carried southward by longshore current (Western Adriatic Coastal Current) (Wang et al., 2007; Bellafiore and Umgiesser, 2010). They were then partially conveyed in the lagoon by the flood tidal current and partially deviated offshore by the jetties of Lido inlet, that interrupt the natural southward coastal drift, thus altering the local sediment dynamics (Molinaroli et al., 2023). Consequently, the inputs of suspended

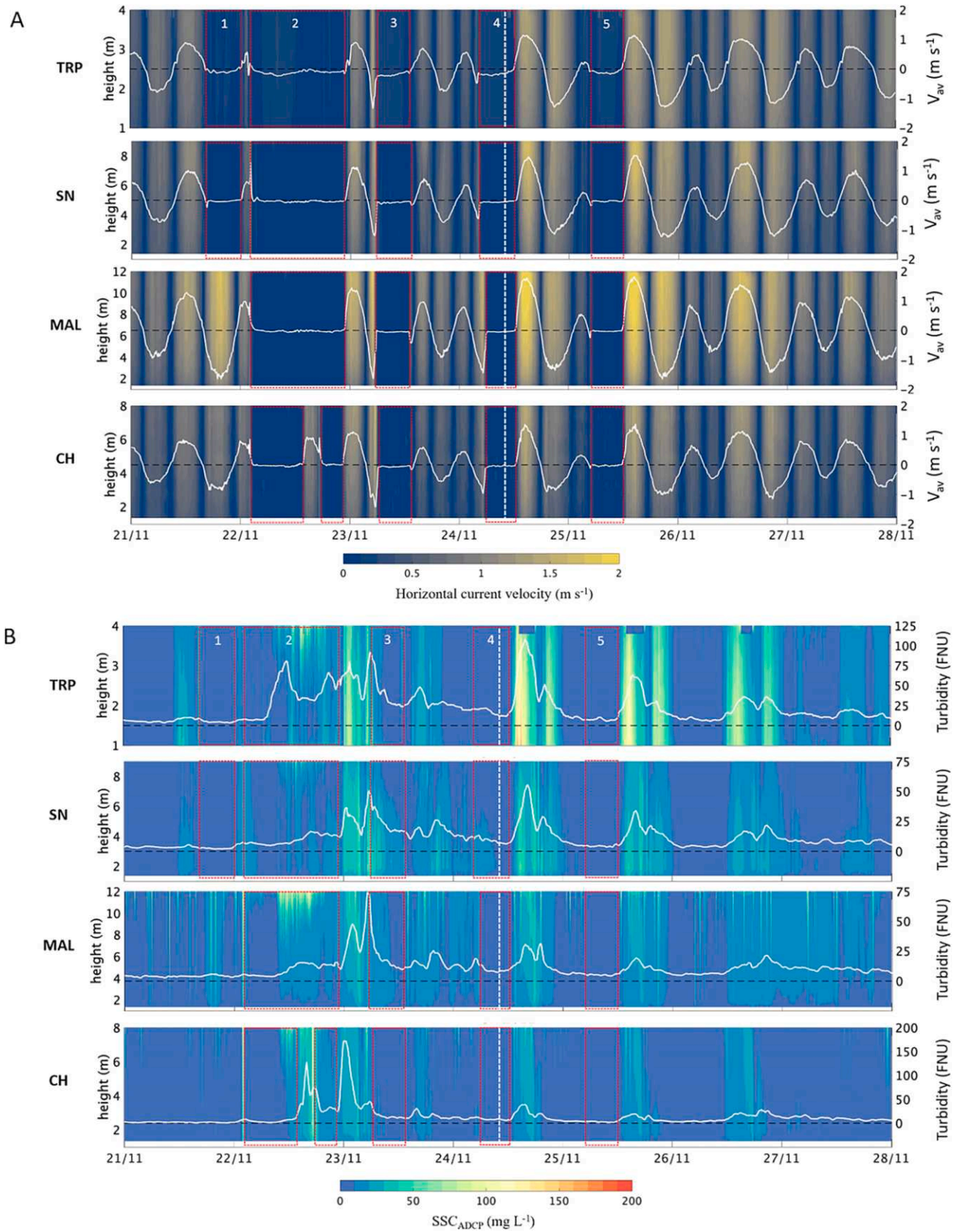

Fig. 7. Panel A: Time series of horizontal current velocity along the water column as height above the ADCPs. White lines in the secondary axis represent v_{av} . Panel B: Time series of suspended sediment concentration along the water column as height above the ADCPs. White lines in the secondary axis represent the T_{OBS} for each inlet. Red dashed boxes on both panels evidence the closure intervals of the MoSE floodgates in each inlet. Vertical dashed white lines mark the S2 satellite overpass time. (For interpretation of the references to color in this figure legend, the reader is referred to the web version of this article.)

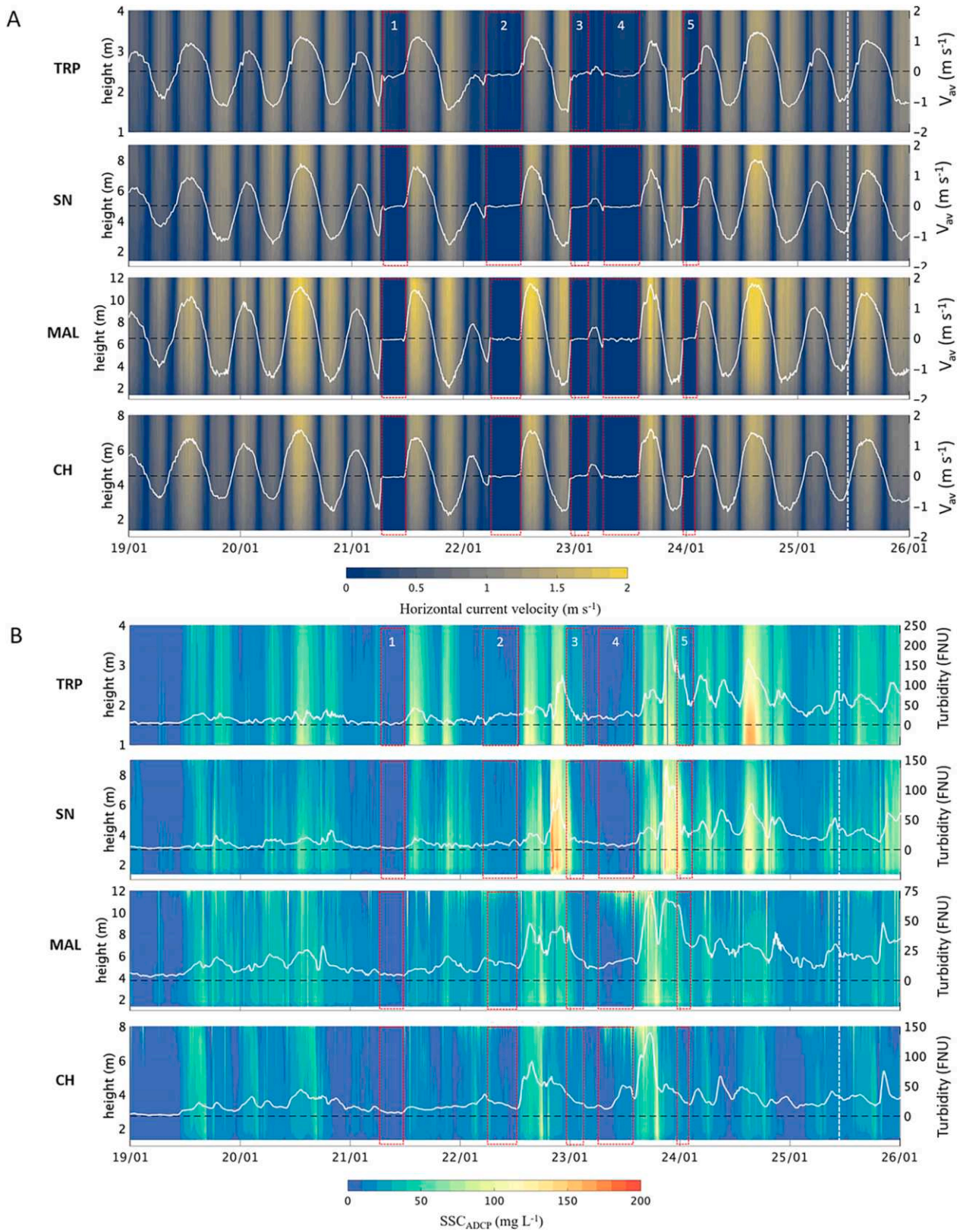

Fig. 8. Panel A: Time series of horizontal current velocity along the water column as height above the ADCPs. White lines in the secondary axis represent v_{av} . Panel B: Time series of suspended sediment concentration along the water column as height above the ADCPs. White lines in the secondary axis represent the T_{OBS} for each inlet. Red dashed boxes on both panels evidence the closure intervals of the MoSE floodgates in each inlet. Vertical dashed white lines mark the S2 satellite overpass time. (For interpretation of the references to color in this figure legend, the reader is referred to the web version of this article.)

sediments at MAL and CH were relatively lower, as shown on Fig. 8A, due to the combined effect of the offshore deviation of the main transport pathway and to the presence of shoreline protections (groins and submerged breakwaters, parallel to the shoreline) at south of the Lido inlet, that inhibit sediment mobilization.

Figs. 9 and 10 present the true-color satellite images (Panel A) and the corresponding T_{SAT} maps (Panel B) from Sentinel-2, captured on November 24th, 2022, and January 25th, 2023, respectively. The synoptic overview of turbidity patterns across the Venice Lagoon and the coastal area of NAS provides insights into both submesoscale and local scale of suspended sediment dynamics. On November 24th, 2022 (Fig. 9), during the satellite overpass, the lagoon was closed and isolated by the MoSE barriers (4th closure, red box in Fig. 7), which are clearly visible in the pseudo true-color image. At this time, the meteo-marine conditions were relatively calm, with wind speeds below 10 m/s in the last 24 h. The T_{SAT} map shows that the NAS was moderately turbid with values ranging from 6 to 18 FNU, as an effect of the meteo-marine conditions of the previous days. According to Braga et al. (2017), the turbidity of NAS in calm conditions typically have a range of 1–3 FNU. The narrow coastal strip, characterized by residual T_{SAT} up to 45 FNU, was originated from the wind-wave resuspension of sediments from the seabed and shorelines by the Bora winds and transported southward (Wang and Pinardi, 2002). The MoSE barriers prevented sea-lagoon exchanges, halting water flow in all inlets and leading to gradual sedimentation of suspended materials within the lagoon also favored by the relatively low winds. Consequently, the T_{SAT} map shows relatively low values within the inlets (14–16 FNU) and in the lagoon (10–15 FNU), with exceptions in the central and northern lagoon basins, where turbidity remains locally higher as an effect of boat traffic, as described by Braga et al. (2020). A moderately higher T_{SAT} is observable in the TRP channel towards the northern lagoon basin (16–20 FNU).

The Sentinel-2 scene, acquired on January 25th, 2023 (Fig. 10, Panel B) during the latest phase of the described storm event, captured the pattern of suspended sediment distribution inside the lagoon and in the coastal areas. The T_{SAT} in the NAS is very high (about 30 FNU) caused by wave-induced resuspension and extended from the coast up to approximately 12 km offshore. The true color image (Panel A) clearly shows the whitecaps of the waves, indicating the active breaking, which determined extremely high T_{SAT} in the nearshore zone (> 200 FNU). Suspended sediments were conveyed in the lagoon by the flood tidal current with different patterns in the inlets, typical of these wind conditions. At the Lido inlet (Fig. 10 B1), the T_{SAT} shows the very turbid coastal belt entrained into the inlet around the northern jetty with a marked asymmetric distribution in the channel. The finer fraction of this suspended load was transported inward at TRP channel along the tidal network up to the marshland areas of the northern lagoon, providing a positive contribution to the morphodynamics. The inputs of particles through the inlets of MAL and CH had lower T_{SAT} than Lido and were limited to the proximity of the flood-tidal delta. Here the jetties intercept the longshore current and only allow the entrance of the offshore suspended fraction. Such significant storm-driven sediment supply was abruptly interrupted during the previous flood phases, when the MoSE barriers were operated.

4.4. Suspended sediment budget

The trend of cumulative suspended sediment load (SSL, tons) through the four inlet channels of the Venice Lagoon is shown in Fig. 11A and B, for the November 2022 and January 2023 events, respectively. The dashed black line indicates the total SSL, obtained as the sum of individual SSL contribution of each inlet. Positive values of SSL indicate seaward transport, while negative values represent material transported into the lagoon. The overall budgets, estimated from the total lagoon SSL by considering an interval that includes the whole event within temporal extremes with coincident water levels at PS, were ~ 13,900 tons for November 2022 and ~ 14,850 tons for January 2023.

In the November 2022 event, the trends of SSL were very similar for the four inlet channels: CH had relatively high variations respect to MAL, SN and TRP channels, with a loss of about ~ 4,720 tons at CH and between 2,700 and 3,360 tons at the other three inlet channels

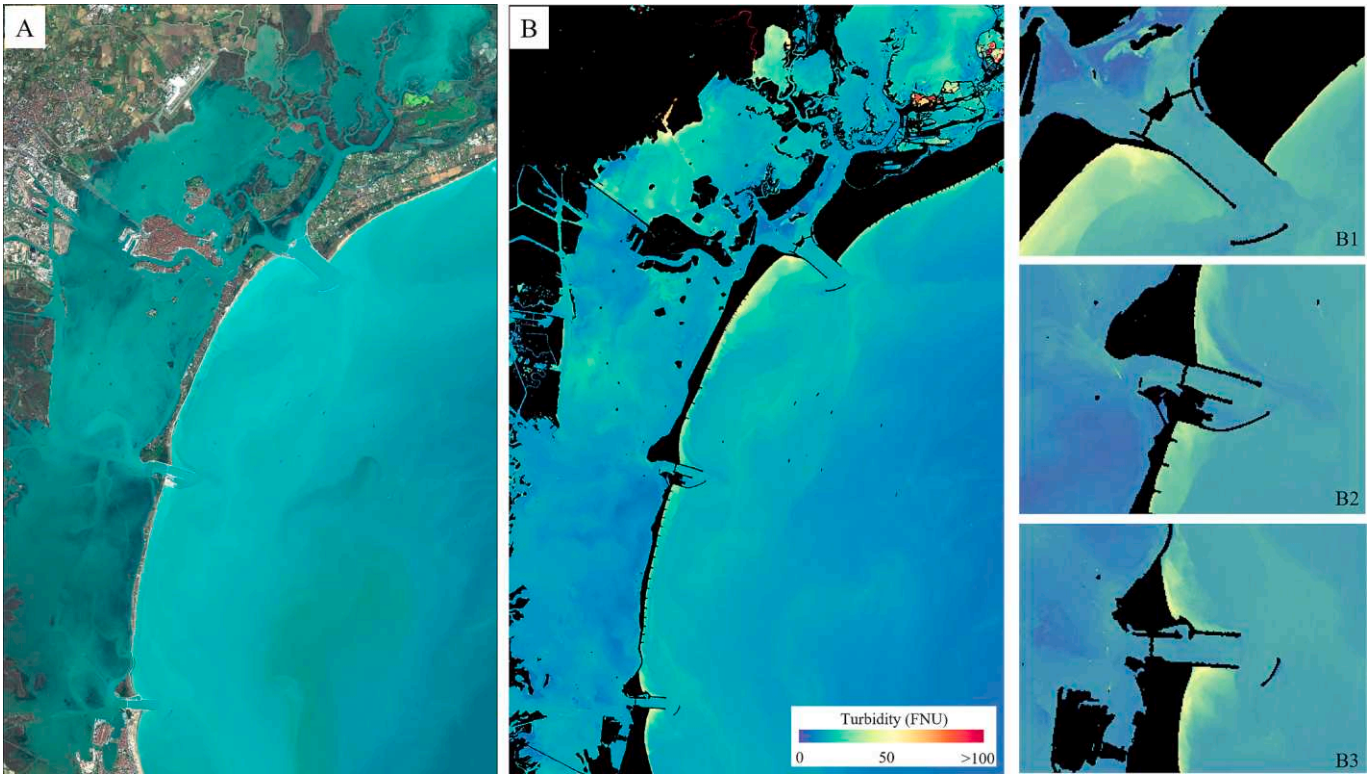

Fig. 9. Panel A: Sentinel-2 true-colour image of the lagoon of Venice acquired on the November 24th 2022 at 10:00 UTC. MoSE barriers closed. Panel B: T_{SAT} map.

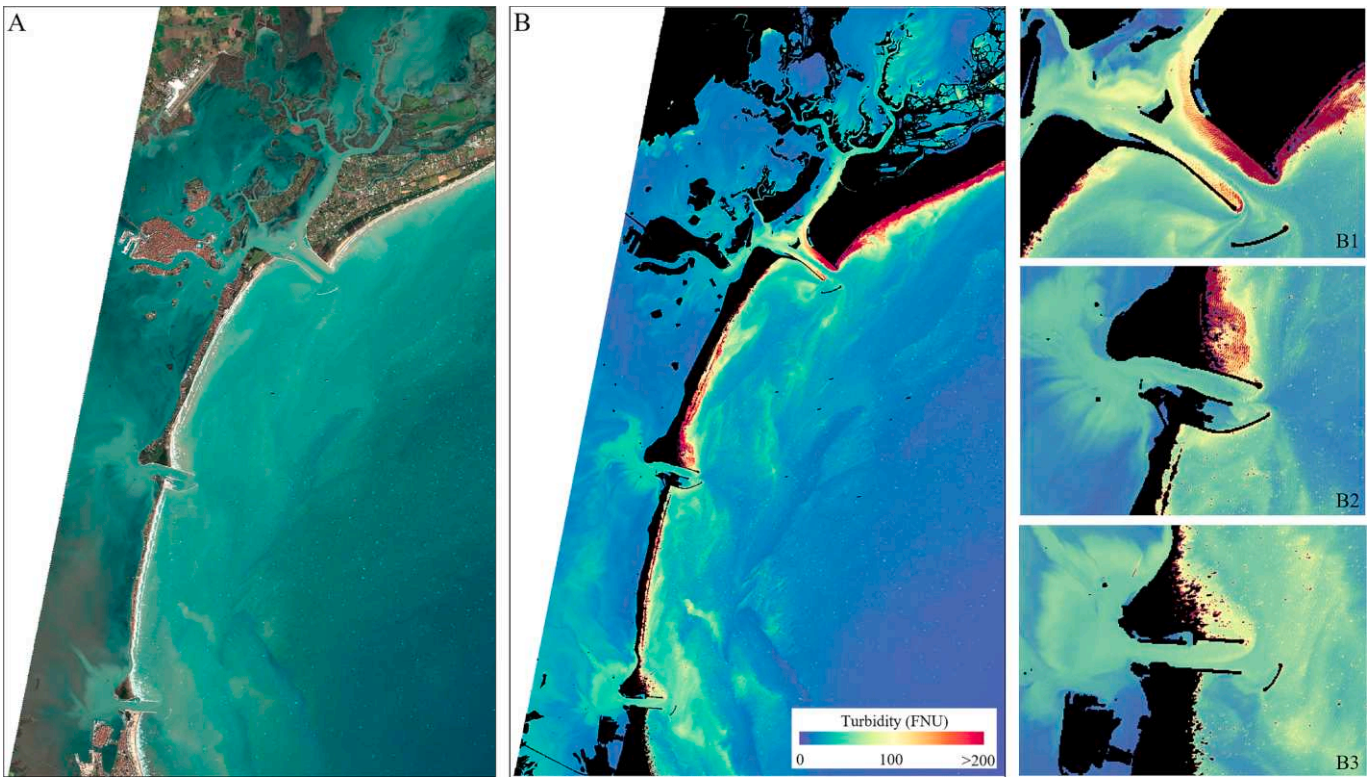

Fig. 10. Panel A: Sentinel-2 true-colour image of the lagoon of Venice acquired on the January 25th January 2023 at 10:00 UTC, late flood phase. Panel B: Sentinel-2-derived T_{SAT} map.

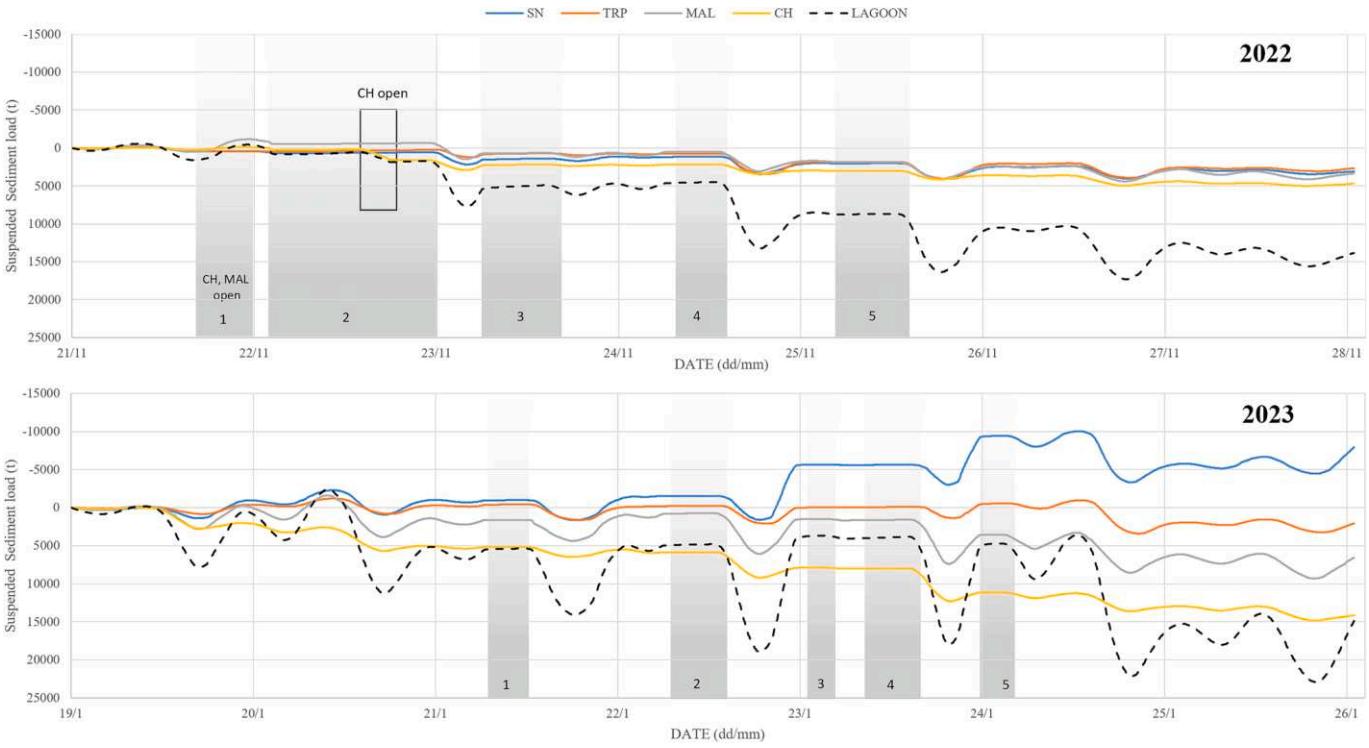

Fig. 11. Cumulative suspended sediment load through the four inlet channels for the investigated periods: Panel A, November 21st to 28th, 2022, Panel B, January 19th to 26th, 2023. The black dashed lines represent the overall exchange for the Venice Lagoon, obtained as the sum of individual SSL contributions. The gray background boxes indicate the MoSE closures.

(Fig. 11A). The marked rise of SSL values, visible for all the inlets, indicated a loss of sediments after every opening of the MoSE barriers, with the onset of ebb tidal currents. These increases were proportional to the residual tidal variations, (i.e., changes in water level) for instance a SSL of 1,272 tons corresponded to the 25 cm excursion in water level that followed the 3rd MoSE operations, while 8,750 and 7,410 tons were related to the excursions of about 1 m in both the 4th and 5th operations, respectively. It should be stressed that, in the following ebb tide, the SSL didn't compensate these consistent exports during the regulated tidal phase, thereby enhancing the asymmetry in the SSL that normally occurred in non-regulated conditions (Defendi et al., 2010). A further forcing affecting the sediment export was the wind-driven resuspension within the lagoon, as in the case of 2nd operation, when the barriers at CH inlet were opened in the period of maximum wind intensity, determining a marked increase of SSL in CH. We can estimate that, in this case, 1150 tons transited through this inlet from the lagoon to the sea. This is the main cause of the shift observed between CH and the other curves in Fig. 11A.

During the January 2023 event, that represents a typical condition of strong northeasterly wind, a marked imbalance is observed between the prevailing net import of suspended sediment in the northern basin (~5,880 tons), resulting from an export of about 2,060 tons at SN and an import of about 7,930 tons at TRP, and the significant export at MAL and CH in the central and southern basins (~6,570 and 14,160 respectively), despite the overall exchange is similar to the one of previous event. As observed from the analysis of SSC_{ADCP} and T_{SAT}, large amounts of suspended sediment were mobilized from the foreshore and nearshore zones of the coast at north of the lagoon of Venice and entered through the Lido inlet with flood tide, while the wind resuspension in the tidal flats of the central and southern lagoon basins determined a prevailing export of materials from MAL and CH during the ebb tidal phase. ADCP-derived loads indicate as the highest export of sediments was measured in non-regulated conditions, although the analysis of T_{SAT} map of January 25th 2023 (Fig. 9B) shows a large amount of suspended sediment transported towards the lagoon along the TRP channel, mainly in its northern edge. This asymmetric distribution, described by Defendi et al. (2010), was not completely measured by the fixed ADCP, that is located on the center-south side of the inlet channel, likely determining an underestimate of SSL at TRP and consequently on the cumulative budget. Moreover, differently from November 2022, in regulated conditions (i.e. the MoSE barriers operations), the overall budget of the 4 inlet channels remained nearly constant (about 5,000 tons), as the losses of sediments in the ebb tide were compensated by the inputs in the flood tide. This suggests that the closures of the MoSE barriers, besides limiting the export, could also affect the budget preventing the input of sediment from the sea, particularly important during Bora events. In combination with the regulation of tidal levels operated by the MoSE system, reduced sediment inputs may exacerbate the erosion of tidal and subtidal morphologies increasing the vulnerability of tidal morphologies in the lagoon wetrlands, due to the acceleration of relative sea level rise (Tosi et al., 2024). The missing sediment inputs from the sea during storms may cause a long-term loss of geomorphic diversity in shallow tidal environments, as showed by Tognin et al. (2022), with eventual cascading effects on biodiversity and ecosystem services typically provided by coastal wetlands (Li et al., 2018). While the Venice lagoon floodgates were built and started to operate, more storm surge barrier projects were recommended and completed worldwide (Orton et al., 2023). All these systems are expected to strongly affect the physics and environmental functions of our coastline and estuaries. Although direct short-term impacts on hydrodynamics and sediment transport of these structures can be easily observed, as shown by this study, long-term changes induced by the barrier operations are harder to predict and require an adequate support by long time series of the variables of interest to improve our understanding of natural system responses and to address protocols and operational strategies for the management of the infrastructures.

5. Conclusions

The monitoring observation system implemented at the inlets of the Venice Lagoon is based on an innovative approach that combines in-situ observations with high temporal resolution from new and existing instrumental platforms and remote sensing techniques. Part of the existing instruments, like the fixed ADCP profilers, were installed and are managed for different purposes and the required technical compromises determined some limitations on the estimate of SSL, as discussed in the previous sections. The resulting dataset enabled us to assess the exchanges of water and sediments between the sea and the lagoon, unraveling the effects of storm surge events on the suspended sediment dynamics under the flow regulations imposed by the activation of MoSE floodgates. The complex interactions between barrier operations and sediment fluxes were analyzed in detail by leveraging the high spatial and temporal resolution of continuous in-situ data and derived parameters, even during adverse weather conditions that would be otherwise prohibitive for on-site work. Although only two cloud-free Sentinel-2 images were available for the periods of interest, satellite-derived products aided the investigation of sediment transport pathways.

The results showed how the exchanges at the inlets under regulated flow can be extremely diversified in response to the specific meteo-marine conditions. In the two investigated events (November 2022 and January 2023), despite the resulting cumulative suspended sediment loads (SSL) were quite similar, the trends of each inlet channel were locally and temporally different. In November 2022, after every opening of the flood barriers, the general export of sediment during ebb tidal phase was not compensated by the import in the flood phase, determining a progressive loss of materials through all the inlet channels. By contrast, during the January 2023 storm event, a marked difference among the exchanges at the inlets was found, with an imbalance between sediment import and export: the import prevailed in the northern basin, while export predominated the southern and central basins. Besides being effective in preventing high waters in Venice, the regulation operated by the barriers can potentially determine short-term positive or negative feedbacks on the lagoon sedimentary budget, minimizing sediment losses from the lagoon or blocking the inputs from the adjacent coast, respectively. An optimal management of the system and criteria for its use in modulating sediment exchanges should be adaptable to the evolution of meteo-marine conditions, also with robust forecast and nowcast modelling tools, that are already available for the Venice Lagoon. This is particularly important in the future climate change scenarios, where the relative sea-level rise will lead to more frequent and longer activations of the floodgates to protect Venice. In the long-term, the expected reduction of lagoon-sea exchanges to protect the human landscape can in fact deeply affect the morphodynamics by exacerbating the loss of habitats in shallow tidal environments of the lagoon, whose preservation is already threatened by natural and anthropogenic pressures. Future research work should be extended over a longer interval, to include the normal-to-moderate meteomarine conditions and the other barrier operations. The time series of water and sediment fluxes at the inlets could be integrated in numerical models to assess the overall budget of the system also considering the effects of tidal flow and wind-wave resuspension inside the lagoon and along the coast.

As a valuable and highly vulnerable environment, the solutions adopted in lagoon of Venice may represent a peculiar case in the context of interventions for the protection of coastal communities by the effects of climate changes. However, actions to preserve the habitat and ecosystem services in the Venice lagoon are just an anticipation of the challenges that we can envisage for similar environments worldwide in the near future where analogous actions will be required. The conceptual approach adopted for the Venice Lagoon can then be fitted to other cases to provide an effective tool for the management of sediment transport and erosion processes in coastal environments, whose

resilience is of growing importance in a changing climate.

CRediT authorship contribution statement

Gian Marco Scarpa: Writing – review & editing, Writing – original draft, Visualization, Methodology, Investigation, Formal analysis, Data curation, Conceptualization. **Silvio Davison:** Writing – review & editing, Visualization, Formal analysis, Data curation. **Giorgia Manfè:** Writing – review & editing, Methodology, Investigation, Formal analysis, Data curation. **Giuliano Lorenzetti:** Methodology, Investigation, Formal analysis, Data curation. **Luca Zaggia:** Writing – review & editing, Project administration, Funding acquisition, Formal analysis, Conceptualization. **Federica Braga:** Writing – review & editing, Project administration, Funding acquisition, Formal analysis, Conceptualization.

Funding

This scientific activity was performed within the Research Programme Venezia2021, coordinated by CORILA, with the contribution of the Provveditorato for the Public Works of Veneto, Trentino Alto Adige and Friuli Venezia Giulia. GMS acknowledges the funding *by the European Union through the Next Generation EU Mission 4 "Education and Research" – Component 2: "From research to business" – Investment 3.1: "Fund for the realisation of an integrated system of research and innovation infrastructures" – Project IR0000032 – ITINERIS – Italian Integrated Environmental Research Infrastructures System – CUP B53C22002150006.*

Declaration of competing interest

The authors declare that they have no known competing financial interests or personal relationships that could have appeared to influence the work reported in this paper.

Acknowledgments

The authors wish to thank the crew of the M/B "Litus", G. Zennaro, R. Vianello, M. Penzo. Time series of flow and acoustic backscatter from bottom-mounted ADCPs were made available by Consorzio Venezia Nuova, the concessionaire of the works for construction of the MoSE mobile barriers at the Venice Lagoon inlets for the Italian Ministry of Public Works. Hydro-meteorological data covering the study area were provided by the Centro Previsione e Segnalazione Maree, Municipality of Venice. The European Space Agency and the European Union's Copernicus program are thanked for the acquisition and free distribution of Sentinel-2 images used in this work. We are grateful to RBINS for making ACOLITE publicly and freely available. The authors acknowledge the facilities of the International Centre for Advanced Studies on River-Sea Systems DANUBIUS-RI in undertaking this research. https://www.danubius-ri.eu/.

The authors also thank the three reviewers for their valuable and significant contributions.

Appendix A. Supplementary data

Supplementary data to this article can be found online at https://doi.org/10.1016/j.jhydrol.2024.132588.

Data availability

Data will be made available on request.

References

Bajo, M., Međugorac, I., Umgiesser, G., Orlić, M., 2019. Storm surge and seiche modelling in the Adriatic Sea and the impact of data assimilation. *Q. J. R. Meteorolog. Soc.* 145 (722), 2070–2084. https://doi.org/10.1002/qj.3544.

Baldassarre, L., Natali, V., De Pascale, F., Vezzi, A., Banchi, E., Bazzaro, M., Relitti, F., Tagliapietra, D., Cibic, T., 2023. The impact of MOSE (Experimental Electromechanical Module) flood barriers on microphytobenthic community of the Venice lagoon. *Microorganisms*. 11 (4), 936. https://doi.org/10.3390/microorganisms11040936.

Bellafiore, D., Umgiesser, G., 2010. Hydrodynamic coastal processes in the North Adriatic investigated with a 3D finite element model. *Ocean Dyn.* 60, 255–273. https://doi.org/10.1007/s10236-009-0254-x.

Braga, F., Zaggia, L., Bellafiore, D., Bresciani, M., Giardino, C., Lorenzetti, G., Maicu, F., Manzo, C., Riminucci, F., Ravaioli, M., Brando, V.E., 2017. Mapping turbidity patterns in the Po river prodelta using multi-temporal Landsat 8 imagery. Estuarine. Coas. Shelf Sci. 198, 555–567. https://doi.org/10.1016/j.ecss.2016.11.003.

Braga, F., Scarpa, G.M., Brando, V.E., Manfè, G., Zaggia, L., 2020. COVID-19 lockdown measures reveal human impact on water transparency in the Venice Lagoon. *Sci. Total Environ.* 736, 139612. https://doi.org/10.1016/j.scitotenv.2020.139612.

Braga, F., Ciani, D., Colella, S., Organelli, E., Pitarch, J., Brando, V.E., et al., 2022. COVID-19 lockdown effects on a coastal marine environment: Disentangling perception versus reality. *Sci. Total Environ.* 817, 153002. https://doi.org/10.1016/j.scitotenv.2022.153002.

Carter, R. W. G., Woodroffe, C. D. (Eds.). *Coastal evolution: Late Quaternary shoreline morphodynamics*. 1994. Cambridge University Press.

Cavaleri, L., Bajo, M., Barbariol, F., Bastianini, M., Benetazzo, A., Bertotti, L., Chiggiato, J., Davolio, S., Ferrarin, C., Magnusson, L., et al., 2019. The October 29, 2018 storm in Northern Italy—An exceptional event and its modeling. Prog. Oceanogr. 178, 102178. https://doi.org/10.1016/j.pocean.2019.102178.

Cooper, J.A.G., Lemckert, C., 2012. Extreme sea-level rise and adaptation options for coastal resort cities: a qualitative assessment from the Gold Coast, Australia. *Ocean Coastal Manage.* 64, 1–14. https://doi.org/10.1016/j.ocecoaman.2012.04.001.

Defendi, V., Kovačević, V., Arena, F., Zaggia, L., 2010. Estimating sediment transport from acoustic measurements in the Venice Lagoon inlets. *Cont. Shelf Res.* 30 (8), 883–893. https://doi.org/10.1016/j.csr.2009.12.004.

Deines, K. L. Backscatter estimation using broadband acoustic Doppler current profilers. In *Proceedings of the IEEE Sixth Working Conference on Current Measurement (Cat. No. 99CH36331). 1999*; 249-253. Doi: 10.1109/CCM.1999.755249.

Dogliotti, A.I., Ruddick, K.G., Nechad, B., Doxaran, D., Knaeps, E., 2015. A single algorithm to retrieve turbidity from remotely-sensed data in all coastal and estuarine waters. *Remote Sens. Environ.* 2015 (156), 157–168. https://doi.org/10.1016/j.rse.2014.09.020.

Favaretto, C., Manfè, G., Volpato, M., Scarpa, G.M., 2022. Effect of Mo. SE closures on wind waves in the Venetian lagoon: in situ and numerical analyses. *Water*. 14 (16), 2579. https://doi.org/10.3390/w14162579.

Ferrarin, C., Cucco, A., Umgiesser, G., Bellafiore, D., Amos, C.L., 2010. Modelling fluxes of water and sediment between Venice Lagoon and the sea. *Cont. Shelf Res.* 30 (8), 904–914. https://doi.org/10.1016/j.csr.2009.08.014.

Ferrarin, C., Bajo, M., Bellafiore, D., Cucco, A., De Pascalis, F., Ghezzo, M., Umgiesser, G., 2014. Toward homogenization of Mediterranean lagoons and their loss of hydrodiversity. *Geophys. Res. Lett.* 41 (16), 5935–5941. https://doi.org/10.1002/2014GL060843.

Ferrarin, C., Tomasin, A., Bajo, M., Petrizzo, A., Umgiesser, G., 2015. Tidal changes in a heavily modified coastal wetland. *Cont. Shelf Res.* 101, 22–33. https://doi.org/10.1016/j.csr.2015.04.002.

Ferrarin, C., Bajo, M., Benetazzo, A., Cavaleri, L., Chiggiato, J., Davison, S., Davolio, S., Lionello, P., Orlic, M., Umgiesser, G., 2021. Local and large-scale controls of the exceptional Venice floods of November 2019. *Prog. Oceanogr.* 197, 102628. https://doi.org/10.1016/j.pocean.2021.102628.

Ferrarin, C., Lionello, P., Orlić, M., Raicich, F., Salvadori, G., 2022. Venice as a paradigm of coastal flooding under multiple compound drivers. Sci. Rep. 12 (1), 5754. https://doi.org/10.1038/s41598-022-09652-5.

Ferrarin, C., Bonaldo, D., Bergamasco, A., Ghezzo, M., 2024. Sea level and temperature extremes in a regulated Lagoon of Venice. *Front. Clim.* 5, 1330388. https://doi.org/10.3389/fclim.2023.1330388.

Gačić, M., Kovačević, V., Mazzoldi, A., Paduan, J., Arena, F., Mosquera, I.M., Gelsi, G., Arcari, G., 2002. Measuring water exchange between the Venetian Lagoon and the open sea. *Eos Trans. AGU*. 83 (20), 217–222. https://doi.org/10.1029/2002EO000147.

Gibbons, S.J.A., Nicholls, R.J., 2006. Island abandonment and sea-level rise: an historical analog from the Chesapeake Bay, USA. *Glob. Environ. Chang.* 16 (1), 40–47. https://doi.org/10.1016/j.gloenvcha.2005.10.002.

Giupponi, C., Bidoia, M., Breil, M., Di Corato, L., Gain, A.K., Leoni, V., Minooei Fard, B., Pesenti, R., Umgiesser, G., 2024. Boon and burden: economic performance and future perspectives of the Venice flood protection system. *Reg. Environ. Chang.* 24 (2), 44. https://doi.org/10.1007/s10113-024-02193-9.

Hersbach, H., Bell, B., Berrisford, P., Hirahara, S., Horányi, A., Muñoz-Sabater, J., Nicolas, J., Peubey, C., Radu, R., Schepers, D., et al., 2020. The ERA5 global reanalysis. *Q. J. R. Meteorolog. Soc.* 146 (730), 1999–2049. https://doi.org/10.1002/qj.3803.

Kombiadou, K., Matias, A., Ferreira, Ó., Carrasco, A.R., Costas, S., Plomaritis, T., 2019. Impacts of human interventions on the evolution of the Ria Formosa barrier island system (S. Portugal). *Geomorphology* 343, 129–144. https://doi.org/10.1016/j.geomorph.2019.07.006.

Leoni, S., Dominik, J., Cassin, D., Manfè, G., Tagliapietra, D., Acri, F., Zonta, R., 2022. Sediment oxygen demand rate in a flow regulated lagoon (Venice, Italy). *Front. Environ. Sci.* 10, 1000665. https://doi.org/10.3389/fenvs.2022.1000665.

Li, X., Bellerby, R., Craft, C., Widney, S.E., 2018. Coastal wetland loss, consequences, and challenges for restoration. *Anthropocene Coasts*. 1 (1), 1–15. https://doi.org/10.1139/anc-2017-0001.

Lionello, P., 2005. Extreme storm surges in the Gulf of Venice: Present and future climate. In *Flooding and Environmental Challenges for Venice and Its Lagoon. In: State of Knowledge*. Cambridge University Press, pp. 59–65. https://hdl.handle.net/11587/111547.

Lionello, P., 2012. The climate of the Venetian and North Adriatic region: Variability, trends and future change. *Phys. Chem. Earth, Parts a/b/c*. 40, 1–8. https://doi.org/10.1016/j.pce.2012.02.002.

Lionello, P., Barriopedro, D., Ferrarin, C., Nicholls, R.J., Orlić, M., Raicich, F., Reale, M., Umgiesser, G., Vousdoukas, M., Zanchettin, D., 2021. Extreme floods of Venice: characteristics, dynamics, past and future evolution. *Nat. Hazards Earth Syst. Sci.* 21, 2705–2731.https://doi.org/10.5194/nhess-21-2705-2021.

Mahdian, M., Hosseinzadeh, M., Siadatmousavi, S.M., Chalipa, Z., Delavar, M., Guo, M., Soroush, A., Noori, R., 2023. Modelling impacts of climate change and anthropogenic activities on inflows and sediment loads of wetlands: case study of the Anzali wetland. *Sci. Rep.* 13 (1), 5399. https://doi.org/10.1038/s41598-023-32343-8.

Mel, R.A., 2021. Exploring the partial use of the Mo. SE system as effective adaptation to rising flood frequency of Venice. *Nat. Hazards Earth Syst. Sci. Discuss.* 1–30. https://doi.org/10.5194/nhess-21-3629-2021.

Mel, R.A., Carniello, L., D'Alpaos, L., 2019. Addressing the effect of the Mo. SE barriers closure on wind setup within the Venice lagoon. *Estuar. Coast. Shelf Sci.* 225, 106249. https://doi.org/10.1016/j.ecss.2019.106249.

Mel, R.A., Coraci, E., Morucci, S., Crosato, F., Cornello, M., Casaioli, M., Mariani, S., Corniello, L., Papa, A., Bonometto, A., Ferla, M., 2023. Insights on the extreme storm surge event of the 22 November 2022 in the Venice Lagoon. *J. Marine Sci. Eng.* 11 (9), 1750. https://doi.org/10.3390/jmse11091750.

Minella, J.P., Merten, G.H., Reichert, J.M., Clarke, R.T., 2008. Estimating suspended sediment concentrations from turbidity measurements and the calibration problem. *Hydrol. Process. Int. J.* 22 (12), 1819–1830. https://doi.org/10.1002/hyp.6763.

Molinaroli, E., Peschiutta, M., Rizzetto, F., 2023. Long-term evolution of an urban barrier island: the case of Venice Lido (Northern Adriatic Sea, Italy). *Water*. 15 (10), 1927. https://doi.org/10.3390/w15101927.

Mullison, J. Backscatter estimation using broadband acoustic doppler current profilers-updated. In *Proceedings of the ASCE Hydraulic Measurements & Experimental Methods Conference, Durham, NH, USA. 2017;* 9-12.

Newton, A., Icely, J., Cristina, S., Brito, A., Cardoso, A.C., Colijn, F., Dalla Riva, S., Gertz, F., Würgler Hansen, J., Holmer, M., et al., 2014. An overview of ecological status, vulnerability and future perspectives of European large shallow, semi-enclosed coastal systems, lagoons and transitional waters. *Estuar. Coast. Shelf Sci.* 140, 95–122. https://doi.org/10.1016/j.ecss.2013.05.023.

Newton, A., Cañedo-Argüelles, M., March, D., Goela, P., Cristina, S., Zacarias, M., Icely, J., 2022. Assessing the effectiveness of management measures in the Ria Formosa coastal lagoon, Portugal. *Front. Ecol. Evolut.* 10, 508218. https://doi.org/10.3389/fevo.2022.508218.

Noe, G.B., Cashman, M.J., Skalak, K., Gellis, A., Hopkins, K.G., Moyer, D., Webber, J., Bentherm, A., Maloney, K., Brakebill, J., et al., 2020. Sediment dynamics and implications for management: State of the science from long-term research in the Chesapeake Bay watershed, USA. *Wiley Interdiscip. Rev. Water*. 7 (4), e1454.

Orton, P., Ralston, D., van Prooijen, B., Secor, D., Ganju, N., Chen, Z., Fernald, S., Brooks, B., Marcell, K., 2023. Increased utilization of storm surge barriers: a research agenda on estuary impacts. *Earth's Future*. 11 (3), e2022EF002991. https://doi.org/10.1029/2022EF002991.

Russ, E., Palinkas, C., 2020. Evolving sediment dynamics due to anthropogenic processes in upper Chesapeake Bay. *Estuar. Coast. Shelf Sci.* 235, 106596. https://doi.org/10.1016/j.ecss.2020.106596.

Scarpa, G.M., Braga, F., Manfè, G., Lorenzetti, G., Zaggia, L., 2022. Towards an integrated observational system to investigate sediment transport in the tidal inlets of the Lagoon of Venice. *Remote Sens. (Basel)*. 14 (14), 3371. https://doi.org/10.3390/rs14143371.

Simpson, M.R., Bland, R., 2000. Methods for accurate estimation of net discharge in a tidal channel. EEE J. Oceanic Eng. 25, 437–445. https://doi.org/10.1109/48.895351.

Tagliapietra, D., Umgiesser, G., 2023. Venice and its lagoon fin de siecle. *Reg. Environ. Chang.* 23 (4), 125. https://doi.org/10.1007/s10113-023-02120-4.

Tognin, D., D'Alpaos, A., Marani, M., Carniello, L., 2021. Marsh resilience to sea-level rise reduced by storm-surge barriers in the Venice Lagoon. *Nat. Geosci.* 14 (12), 906–911. https://doi.org/10.1038/s41561-021-00853-7.

Tognin, D., Finotello, A., D'Alpaos, A., Viero, D.P., Pivato, M., Mel, R.A., Defina, A., Bertuzzo, E., Marani, M., Carniello, L., 2022. Loss of geomorphic diversity in shallow tidal embayments promoted by storm-surge barriers. *Sci. Adv*. 8 (13), eabm8446. https://doi.org/10.1126/sciadv.abm8446.

Tosi, L., Da Lio, C., Cosma, M., Donnici, S., 2024. Vulnerability of tidal morphologies to relative sea-level rise in the Venice Lagoon. *Sci. Total Environ.* 931, 173006. https://doi.org/10.1016/j.scitotenv.2024.173006.

Umgiesser, G., 2020. The impact of operating the mobile barriers in Venice (MOSE) under climate change. *J. Nat. Conserv*. 54, 125783. https://doi.org/10.1016/j.jnc.2019.125783.

Vanhellemont, Q., 2019. Adaptation of the dark spectrum fitting atmospheric correction for aquatic applications of the Landsat and Sentinel-2 archives. *Remote Sens. Environ.* 225, 175–192. https://doi.org/10.1016/j.rse.2019.03.010.

Vanhellemont, Q., Ruddick, K., 2018. Atmospheric correction of metre-scale optical satellite data for inland and coastal water applications. *Remote Sens. Environ.* 216, 586–597. https://doi.org/10.1016/j.rse.2018.07.015.

Wang, X., Pinardi, N., Malacic, V., 2007. Sediment transport and resuspension due to combined motion of wave and current in the northern Adriatic Sea during a Bora event in January 2001: a numerical modelling study. *Cont. Shelf Res.* 27, 613–633. https://doi.org/10.1016/j.csr.2006.10.008.

Webster, I.T., 2011. Dynamic assessment of oceanic connectivity in a coastal lagoon—the Coorong, Australia. *J. Coastal Res.* 27 (1), 131–139. https://doi.org/10.2112/JCOASTRES-D-10-00079.1.

Zarotti, G., 2022. MOSE: The Defence System to Safeguard Venice and Its Lagoon. In: *Imagine Math 8: Dreaming Venice*. Springer, Cham, pp. 41–53. https://doi.org/10.1007/978-3-030-92690-8_4.